

## Adsorption of Reactive Blue 5G Dye by Activated Carbon and Pyrolyzed Shale Oil Residue<sup>†</sup>

Rafael Lambrecht<sup>1</sup>, Maria Angélica S.D. Barros<sup>1\*</sup>, Eneida S. Cossich<sup>1</sup>, Edson A. Silva<sup>2</sup>, Gleisy Kelly L. Matta<sup>1</sup> and Rosalvo Stachiw<sup>3</sup> (1) Departamento de Engenharia Química, Universidade Estadual de Maringá, Av. Colombo 5790, Bloco D-90, Maringá-PR, Brazil. (2) Universidade Estadual do Oeste do Paraná, Rua da Faculdade 645, Jardim La Salle, Toledo-PR, Brazil. (3) Universidade Tecnológica Federal do Paraná, Rua 7 de Setembro 3165, Centro, Curitiba-PR, Brazil.

**ABSTRACT:** This work was aimed at the study of the adsorption mechanism of Reactive Blue 5G dye on activated carbon derived from babassu shells and pyrolyzed oil shale residue. Experiments were undertaken employing a fixed bed reactor at 30°C using continuous systems. To minimize diffusional resistances, the influence of the flow rate was investigated via breakthrough curves at a feed concentration of 35 mg/l. Breakthrough curves for flows in the range 2–10 ml/min were carried out using bed height of 15.5 cm for activated carbon and 9.5 cm for pyrolyzed oil shale residue, with an inlet diameter of 1.01 cm. From the calculated mass-transfer parameters, it was shown that the minimum resistance to flow occurred at 4 ml/min for activated carbon and at 2 ml/min for pyrolyzed oil shale residue. It was concluded that the sizes of the pores in the adsorbents play an important role in the adsorption mechanism.

### 1. INTRODUCTION

Dyes are one of the major constituents of wastewaters produced from many industries related to textile, paint and varnishes, plastics, tannery, etc. Coloured dye effluents pose a major threat to the surrounding ecosystem. Of such dyes, Reactive Blue 5G is a well-known Reactive dye which is mainly used in textile industries. The resulting textile wastewater is characterized by a deep blue colour which affects the nature of water by inhibiting the penetration of sunlight, and thus reduces photosynthetic action. Hence, there is a considerable need to treat such effluents prior to discharge.

Adsorption has been shown to be a good method for the removal of coloured contaminants as it offers a very simple and sludge-free operation. The use of activated carbons in such adsorption processes provides the best method for colour removal from wastewater (Rozzi *et al.* 1995). However, to provide any economic benefit, the starting materials should be as cost-effective as possible. Such possible benefit could be the use of activated carbons made from babassu shells which are very abundant in the northeast of Brazil (Jaguaribe *et al.* 2005).

Another waste material that deserves attention is oil shale residue whose ash can be obtained as an inorganic residue from the direct combustion of shale oil used as a source of energy. The total residual ash material that might be generated from shale oil reserves has been estimated to be

<sup>†</sup>First presented at the 6th Brazilian Meeting on Adsorption held in Maringá, State of Paraná, Southern Brazil on August 13–16, 2006.

\*Author to whom all correspondence should be addressed. E-mail: angelica@deq.uem.br.

ca.  $3.2 \times 10^{11}$  tonnes and such waste material could be applied as an adsorbent (Al-Qodah 2002). Another residue is the pyrolyzed oil shale residue generated in the pyrolysis of shale oil, a process known commercially as PETROSIX/PETROBRAS. This material is produced at the rate of ca. 6600 tonne/d and has been investigated as an adsorbent of organic substances (Stachiw 2005).

Most studies of the adsorption of dyes have been conducted using batch systems, but continuous processes are often applied in wastewater treatment. Unfortunately, the uptake process in a continuous system may not follow the mechanism of the batch system (Barros *et al.* 2004). Consequently, investigations of the best operational conditions in fixed bed systems need to be undertaken to overcome this lack of information. Hence, the present work was aimed at analyzing the operational conditions that would minimize the mass-transfer resistances encountered by Reactive Blue 5G dye when adsorbed by activated carbon derived from babassu shells and from pyrolyzed oil shale residue.

## 2. EXPERIMENTAL

### 2.1. Materials

The synthetic effluent utilized for the runs was prepared using Reactive Blue 5G dye whose molecular structure is shown in Figure 1. The concentration of dye in solution was measured via a Shimadzu UV-1601PC UV-vis spectrophotometer at a wavelength of 610 nm. In order to calculate the longitudinal length of the dye molecule, use was made of the semi-empirical calculus (AM1) from GAUSSIAN 03 software.

The activated carbon derived from babassu shells with a particle diameter of 0.56 mm was kindly donated by Tobasa Bioindustrial, while the pyrolyzed oil shale residue with a particle diameter of 0.22 mm was obtained from PETROSIX/PETROBRAS. Both samples were characterized by  $N_2$  adsorption, measurements of their zero point of charge (zpc) (Guilarduci *et al.* 2006) and infrared spectroscopy.

### 2.2. Activated carbon and pyrolyzed oil shale residue fixed beds

The experimental arrangement for performing adsorption studies is shown schematically in Figure 2. The adsorption column consisted of a clear glass tube (1.01 cm i.d., 30 cm length) containing the adsorbent (granular activated carbon or pyrolyzed oil shale residue) supported by glass beads. The column was connected to a heat-exchanger that maintained the system at

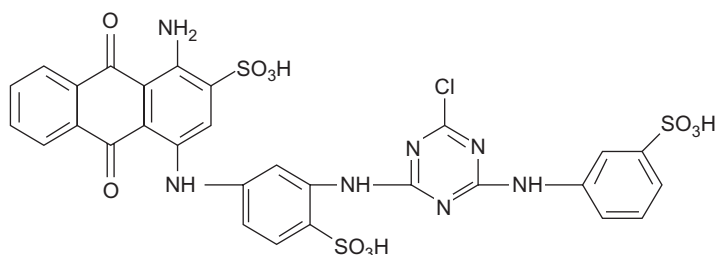


**Figure 1.** The molecular structure of Reactive Blue 5G dye (Koprivanac *et al.* 2005).

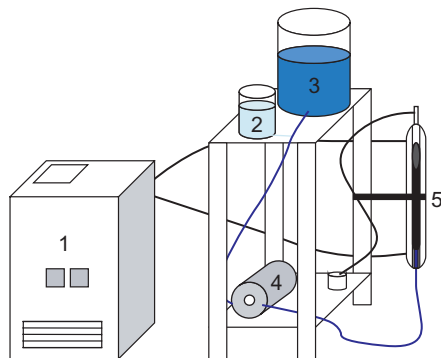


**Figure 2.** Experimental set-up for dynamic adsorption studies: 1, heat exchanger; 2, de-ionized water tank; 3, dye solution tank; 4, pump; 5, adsorption column.

30°C. Before the commencement of any runs, the activated carbon or pyrolyzed oil shale residue beds were rinsed by pumping de-ionized water upwards through the column to remove air bubbles. After adjusting the bed height at 15.5 cm for the activated carbon (5.639 g) or 9.5 cm for the pyrolyzed oil shale residue (7.264 g), the column was completed with glass beads. The adsorption process was commenced by pumping the dye solution into the column in an upward direction. For the evaluation of the best operational conditions, the experimental data were obtained with a feed concentration of 35 mg/l and flow rates of 2, 4, 6, 8 and 10 ml/min. Samples were collected regularly at the column outlet. Additional COD analysis was conducted with the packed bed containing pyrolyzed oil shale residue as some organics could have been present in this case. Although de-ionized water was employed for washing the column during the packing step, the amount of such water in the system was negligible ( $\cong 30$  mg/l) when adsorption commenced. All breakthrough curves ( $C/C_0$  versus  $t$ ) were plotted taking into account the dye concentration in the outlet samples as a function of the running time until the column was saturated. It was assumed that the breakpoint was reached when the outlet concentration was 1 mg/l.

### 2.3. Estimation of the mass-transfer parameters

The dimensionless time of the breakthrough curves may be defined as (McCabe *et al.* 2001):

$$\tau = \frac{1}{\rho_p (1 - \varepsilon) H (W_{\text{sat}} - W_0)} u_0 C_0 \left( t - H \frac{\varepsilon}{u_0} \right) \quad (1)$$

where  $H\varepsilon/u_0$  is the time required to displace fluid from the bed voids (normally negligible) and  $u_0 C_0 t$  is the total solute fed into unit cross-section of bed up to time  $t$ . The time  $t$  can be considered as the time equivalent to fill the usable capacity of the bed ( $t_u$ ) up to the break-point time ( $t_b$ ) (Barros *et al.* 2003), the latter being defined as the time when the effluent concentration ( $C$ ) reaches 1 mg/l. The term  $\rho_p (1 - \varepsilon) H (W_{\text{sat}} - W_0)$  is the capacity of the bed, or the amount of solute exchanged if the entire bed came to equilibrium with the feed, i.e. the time equivalent to the total stoichiometric capacity of the packed bed ( $t_l$ ) (Geankoplis 1993).

Thus, equation (1) can be simplified to (Pereira *et al.* 2006):

$$\tau = \frac{t_u}{t_t} \quad (2)$$

If the entire bed attains equilibrium, the mass balance in the column provides the values of  $t_u$  and  $t_t$  (Geankoplis 1993):

$$t_u = \int_0^{t_b} \left(1 - \frac{C}{C_0}\right) dt \quad \text{and} \quad t_t = \int_0^{\infty} \left(1 - \frac{C}{C_0}\right) dt \quad (3)$$

The dimensionless time  $\tau$  is the fraction of the total bed capacity or length utilized up to the breakthrough (Geankoplis 1993). Hence, the length of unused bed is:

$$H_{\text{UNB}} = (1 - \tau)H \quad (4)$$

where  $H_{\text{UNB}}$  represents the mass-transfer zone (MTZ). Small values of this parameter mean that the breakthrough curve is close to an ideal step with negligible mass-transfer resistance.

Another parameter that should be considered for column evaluation is the average residence time ( $\bar{t}$ ). From probability principles, the average residence time of a fluid element may be written as:

$$\bar{t} = \int_0^{\infty} t dF(t) \quad (5)$$

with  $F(t)$  being equivalent to  $C/C_0$  for breakthrough curves.

An indirect measure of how far the column operates from the optimum operating conditions is the operational ratio (Pereira *et al.* 2006) that is given by:

$$R_0 = \frac{1}{t_u} |\bar{t} - t_u| \quad (6)$$

Values of the operational ratio close to zero indicate that the residence time of the fluid in the packed bed ( $\bar{t}$ ) is similar to the time desirable in the column ( $t_u$ ). In such cases, the column operates close to the optimal region of operation (Pereira *et al.* 2006).

From the average residence time it is also possible to evaluate the dimensionless variance of the breakthrough curve (Hill 1977), which is given by:

$$\sigma_{\theta}^2 = \frac{1}{\bar{t}^2} \left[ \int_0^{\infty} t^2 \left( \frac{dF(t)}{dt} \right) dt - \bar{t}^2 \right] \quad (7)$$

This parameter, initially applied for non-ideal reactors, has now also been applied in adsorption processes to estimate the dispersion in the packed bed. Values of  $\sigma_{\theta}^2 \approx 0$  mean that the packed bed behaves close to an ideal plug flow with negligible axial dispersion and small mass-transfer resistance (Hill 1977). It should be noted that, in adsorption processes, the dimensionless variance can reach values greater than one, as a consequence of the degree of dispersion in the sorption column.

The bed performance for Reactive Blue 5G dye uptake is well demonstrated by the breakthrough capacity of the column, with  $U_{\text{dye}}^{\text{t}}$  being defined as the amount of dye adsorbed prior to the breakpoint ( $C = 1 \text{ mg}/\ell$ ). Integration of the areas under the breakthrough curve gives the amount of dye not recovered by the adsorbent, based on the difference in the quantity of dye fed to the column. This value allows the amount retained by the adsorbent to be determined (Valdman *et al.* 2001).

### 3. RESULTS AND DISCUSSION

According to AM1 from GAUSSIAN 03, the longitudinal length of the Reactive Blue 5G dye molecule is 22.35 Å while the average diameter may be estimated as 9 Å.

The BET area of the activated carbon was 816  $\text{m}^2/\text{g}$  while its micropore surface area was 1160  $\text{m}^2/\text{g}$ . This indicates that the material had a predominantly microporous structure with an average diameter (BJH) of 20.46 Å. The point of zero charge (pzc) of the carbon sample occurred at  $\text{pH} \approx 7.7$ . This indicates that the surface of this adsorbent was positively charged under acidic conditions, while at pH values above 7.7 it was negatively charged. Since the dye has three sulphonic groups in its structure capable of dissociation under acidic conditions, this indicates that solutions with pH values in the range 5.5–6.5 would favour dye adsorption.

The infrared spectrum of the activated carbon sample is displayed in Figure 3(a). The presence of peaks at wavelengths of ca. 3200–3600  $\text{cm}^{-1}$  demonstrates the existence of carboxylic groups in the sample, whereas the peaks in the wavelength region of ca. 1000–1200  $\text{cm}^{-1}$  indicate the existence of phenolic, lactonic and ether groups. Some peaks related to C=O bonds also occur at wavelengths in the range ca. 2250–2400  $\text{cm}^{-1}$  (Pradhan and Sandle 1999). Due to the large number of groups on the surface of the adsorbent, it is possible that the dye can be adsorbed on these groups as well as via a physisorption process. This supposition is in agreement with that arising from previous work (Attia *et al.* 2006).

The BET surface area of the pyrolyzed oil shale residue was 13.65  $\text{m}^2/\text{g}$ , with the sample having a predominantly mesoporous structure. Such a feature could facilitate the diffusion process and

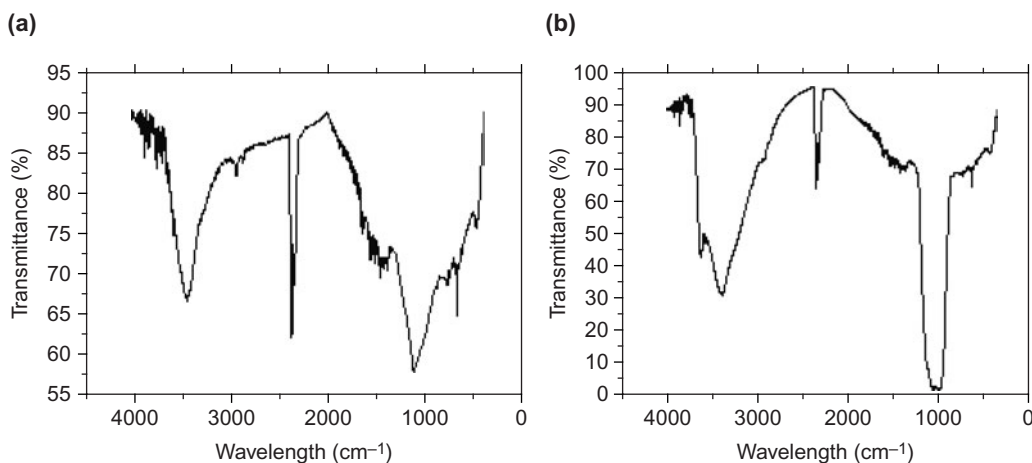
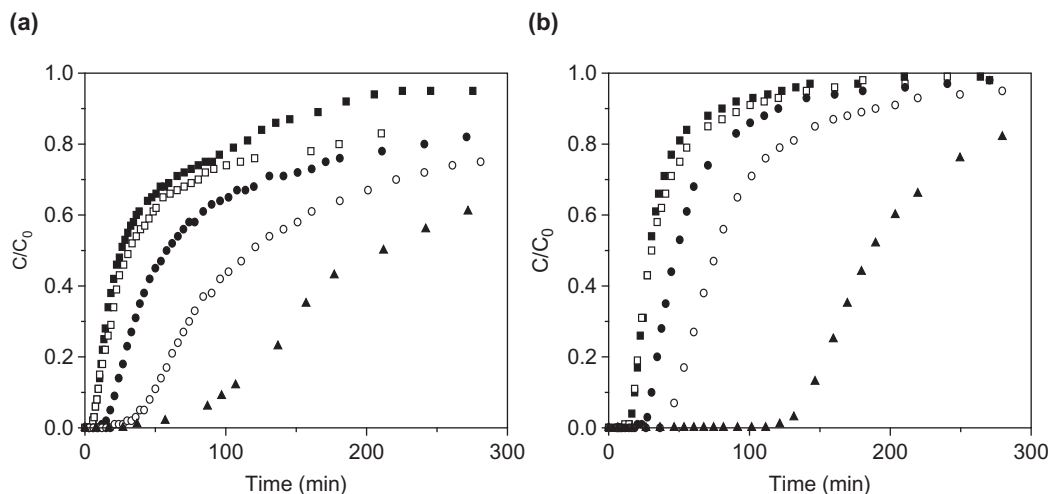


Figure 3. FT-IR spectrum of activated carbon derived from (a) babassu shells and (b) pyrolyzed shale oil residue.

adsorption on available sites within the interior of the structure. On the other hand, the pzc for this sample was 6.3, which is close to the upper limit of the solution pH range studied (6.5). This suggests that it may be difficult to retain some adsorbate molecules if the feed solution has a pH range of 6.3–6.5. Figure 3(b) shows the FT-IR spectrum of the pyrolyzed shale oil residue. This exhibits more pronounced peaks than that for the activated carbon, with carboxylic groups being present in the 3200–3600  $\text{cm}^{-1}$  range. Peaks related to C=O may also be observed in the 2250–2400  $\text{cm}^{-1}$  range, as well as some nitrate complexes and aromatics (1500–1600  $\text{cm}^{-1}$ ). The presence of large peaks in the 1000–1200  $\text{cm}^{-1}$  range also suggests the existence of surface groups such as phenols, ethers or lactones at a higher content than in the activated carbon sample.

Figure 4(a) shows the breakthrough results for flow rates in the range 2–10  $\text{mL}/\text{min}$  and a feed concentration of 35  $\text{mg}/\ell$  on the activated carbon bed. Similarly, Figure 4(b) presents the breakthrough results for the pyrolyzed oil shale residue bed. It will be seen that, in both cases, changing the flow rate over the range studied led to huge differences in the uptake mechanism for the dye molecules.

Firstly, it will be seen that the shape of the uptake curves was hardly influenced by the nature of the adsorbent, although the microporous activated carbon exhibited a considerable uptake up to 3000 min while the mesoporous shale oil residue provided a much smaller uptake up to 500 min. To allow a clearer view of the uptake process with both adsorbents, the saturation points of all the breakthrough curves are not presented in Figure 4. A lengthy saturation process arises from the steric problems experienced by a large molecule when diffusing into a microporous or a mesoporous system. Moreover, since the size of the Reactive Blue 5G dye molecule in a transverse position was approximately equal to that of the micropores of the activated carbon, such molecules would not be adsorbed to any great extent as they would be too large to be accommodated within the pore. However, the molecule could be accommodated in a longitudinal orientation, since its average transverse diameter was 9 Å. The orientation adopted by the Reactive Blue 5G dye molecule when it is adsorbed in the pores of the shale oil residue is not important in the diffusion process, as the pores in both adsorbents were sufficiently large to exhibit only small



**Figure 4.** Breakthrough curves for  $C_0 = 35 \text{ mg}/\ell$ : (a) activated carbon from babassu shells; (b) pyrolyzed shale oil residue. Data points relate to the following flow rates: ■, 10  $\text{mL}/\text{min}$ ; □, 8  $\text{mL}/\text{min}$ ; ●, 6  $\text{mL}/\text{min}$ ; ○, 4  $\text{mL}/\text{min}$ ; ▲, 2  $\text{mL}/\text{min}$ .

diffusional resistances. The result of these textural properties was a smooth shape towards saturation in the activated carbon breakthrough curves, whereas a steeper type of saturation was observed in the breakthrough curves on the shale oil residue. In fact, smoother curves and longer tails are characteristic of mass-transfer zones with an extended length, as is indicated by the data recorded in Table 1.

This table presents the quantitative results for the breakthrough curves for the activated carbon as presented in Figure 4(a). It can be seen that a flow rate of 4 mL/min provided minimum values for the length of the mass-transfer zone (MTZ) and  $R_0$ , together with the maximum value for  $U_{dye}^u$ . The magnitude of the  $\sigma_\theta^2$  parameter is also a maximum under these circumstances, indicating that, in this case, the more dispersed the dye, the better will be its adsorption — probably as a result of the interaction between the large dye molecule and the micropores of the adsorbent as discussed above. Hence, a flow rate of 4 mL/min provided the best operational conditions of all the various flows studied.

Table 2 presents the quantitative results of the breakthrough curves for the pyrolyzed oil shale residue as presented in Figure 4(b). It can be seen that, in this case, a flow rate of 2 mL/min led to a minimum value for MTZ,  $R_0$  and  $\sigma_\theta^2$ , and the maximum value for  $U_{dye}^u$ . Hence, a flow rate of 2 mL/min provided the best operational conditions of all the various flows studied in this case. It will be noted that the magnitude of the dimensionless variance,  $R_0$ , was much lower than for adsorption onto the babassu activated carbon, indicating that the large amount of mesopores present in the structure of the pyrolyzed oil shale residue facilitate the diffusion of the dye molecule. Aggregation of the dye in aqueous solution (Dakyki and Nemcova 1999) hardly

**TABLE 1.** Mass-transfer Zone (MTZ) Length and Reactive Blue 5G Dye Uptake Parameters for Fixed Bed Adsorption onto Activated Carbon

Flow rate (mL/min)	MTZ (cm)	$R_0$	$\sigma_\theta^2$	$U_{dye}^u$ (mg/g)
10.0	14.07	0.94	6.4	0.39
8.0	14.43	0.96	2.0	0.31
6.0	14.21	0.95	7.6	0.57
4.0	13.94	0.92	8.6	0.88
2.0	14.35	0.96	6.4	0.77

**TABLE 2.** Mass-transfer Zone (MTZ) Length and Reactive Blue 5G Dye Uptake Parameters for Fixed Bed Adsorption onto Pyrolyzed Oil Shale Residue

Flow rate (mL/min)	MTZ (cm)	$R_0$	$\sigma_\theta^2$	$U_{dye}^u$ (mg/g)
10.0	7.038	0.747	0.890	0.54
8.0	6.534	0.700	1.227	0.58
6.0	5.873	0.623	1.011	0.75
4.0	5.909	0.622	0.792	0.77
2.0	4.268	0.463	0.511	1.23

influences the adsorption process. The surface groups which are responsible for adsorption onto the activated carbon are also located within the mesopores of the pyrolyzed oil shale residue, so that although the dye molecules will continue to be attracted electrostatically to the adsorbent surface they will also be adsorbed successfully in the mesopores. This fact explains the larger amounts of dye retained by the pyrolyzed oil shale residue, in addition to the lower values of the dimensionless variance for this adsorbent.

Since the surface groups are more accessible in the mesopores and the influence of aggregation of the dye molecules is negligible, this leads a higher of uptake of dye by the pyrolyzed oil shale residue at the breakpoint. It may also be observed that this adsorbent had a lower pzc value which was close to the lower value of the solution pH employed. It is possible that some dye molecules may have been repelled as a result of the negative charges on the adsorbent surface as well as those associated with the dye molecule under these circumstances, but fortunately this was not a pronounced effect and did not interfere with the high sorption of the dye molecule.

Finally, it should be recalled that both adsorbents were derived from natural sources and that the data presented are the average of the experimental results obtained. Bearing these facts in mind, it may therefore be concluded that both adsorbents retained dye molecules and they may be applied in wastewater treatments when a high efficiency is not required.

#### **4. CONCLUSIONS**

The main conclusions derived from the results presented in the present work may be summarized as follows:

1. The activated carbon exhibited pronounced microporosity with some surface groups capable of dye adsorption, while the pyrolyzed oil shale residue was basically a mesoporous material. Such differences had a considerable influence on the adsorption process of a large molecule such as that of Reactive Blue 5G dye.
2. The uptake mechanism in both adsorbents occurred with a dimensionless variance less than one, due to the steric problems faced by the large dye molecule in its diffusion into the adsorbent structures and its attachment at suitable adsorption sites.
3. The optimized conditions were 2 mL/min for the up-flow pyrolyzed oil shale residue fixed bed and 4 mL/min for the up-flow activated carbon fixed bed when both were accommodated within a column of 1.01 cm i.d. operated at 30°C. With such flow rates, it was found that the length of the unused bed was small and that the operation ratios and breakthrough capacities of the column were high.
4. A comparison of the efficiency of both adsorbents led to the conclusion that pyrolyzed oil shale residue was more efficient for dye uptake due to the presence of mesoporosity, with the dye molecules experiencing less diffusional problems in this case.

#### **ACKNOWLEDGEMENTS**

The authors are grateful to the Conselho Nacional de Desenvolvimento Científico e Tecnológico (CNPq) for financial assistance, the Department of Chemistry of the State University of Londrina (DQI/UUEL) for the infrared spectroscopy analyses, and Tobasa Bioindustrial de Babassu S.A. and PETRSIX/PETROBRAS for the adsorbents studied.



## REFERENCES

- Al-Qodah, Z. (2002) *Water Res.* **34**, 4295.
- Attia, A.A., Rashwan, W.E. and Khedr, S.A. (2006) *Dyes Pigm.* **69**, 128.
- Barros, M.A.S.D., Silva, E.A., Arroyo, P.A., Tavares, C.R.G., Schneider, R.M., Suszek, M. and Sousa-Aguiar, E.F. (2004) *Chem. Eng. Sci.* **59**, 5959.
- Barros, M.A.S.D., Zola, A.S., Arroyo, P.A., Sousa-Aguiar, E.F. and Tavares, C.R.G. (2003) *Braz. J. Chem. Eng.* **20**, 413.
- Dakyki, M. and Nemcova, I. (1999) *Dyes Pigm.* **40**, 141.
- Geankoplis, C.J. (1993) *Transport Processes and Unit Operations*, 3rd Edn, Prentice Hall Publishers, Upper Saddle River, NJ, U.S.A.
- Guilarduci, V.V.S., Mesquita, J.P., Martelli, P.B. and Gorgulho, H.F. (2006) *Quím. Nova* **29**, 1226.
- Hill, C.G. (1977) *An Introduction to Chemical Engineering Kinetics and Reactor Design*, John Wiley & Sons, New York.
- Jaguaribe, E.F., Medeiros, L.L., Barreto, M.C.S. and Araujo, L.P. (2005) *Braz. J. Chem. Eng.* **22**, 41.
- Koprivanac, N., Kusic, H., Vusevi, D., Peternel, I. and Locke, B.R. (2005) *J. Hazard. Mater.* **117**, 113.
- McCabe, W.L., Smith, J.C. and Harriot, P. (2001) *Unit Operations of Chemical Engineering*, 6th Edn, McGraw-Hill International, New York.
- Pereira, M.R., Arroyo, P.A., Barros, M.A.S.D., Sanches, V.M., Silva, E.A., Fonseca, I.M. and Lovera, R.G. (2006) *Adsorption* **12**, 155.
- Pradhan, B.K. and Sandle, N.K. (1999) *Carbon* **37**, 1323.
- Rozzi, A., Malpei, F., Bonomo, L. and Bianchi R. (1995) *Water Sci. Technol.* **39**, 121.
- Stachiw, R. (2005) *Qualifying Doctorate*, UTFPR.
- Valdman, E., Erijman, L., Pessoa, F.L.P. and Leite, S.G.F. (2001) *Process Biochem.* **36**, 869.

